Proceedings of ICFDP7:
International Conference on Fluid Dynamics and Propulsion
December 18-20, 2001, Cairo, Egypt

ICFDP7-2001041

A PARAMETRIC STUDY OF AXISYMMETRIC SWIRLING FLOWS IN A LOW APSECT RATIO VORTEX CHAMBER

Wahid S. Ghaly[1] Georgios H. Vatistas[2]
Concordia University
Mechanical and Industrial Engineering Department
1455 de Maisonneuve West, Montreal, Quebec, CANADA H3G 1M8
[1]Associate Professor
[2]Professor

ABSTRACT

The flow in a low aspect ratio vortex chamber can be modeled as a flow between two closely spaced concentric disks. The flow is assumed to be axisymmetric swirling and flowing radially inward. A novel numerical method is used to solve this flow assuming steady laminar incompressible fluid flow. The Navier-Stokes equations are cast in terms of the radius times the radial velocity rV_r, and the radius times the tangential velocity rV_θ, in cylindrical coordinates. The coupled equations are solved simultaneously using the shooting method coupled with Newton's method; numerical integration is carried out using the Runge-Kutta method. A parametric study is carried out to demonstrate the effect of the Reynolds and swirl numbers on the flow and pressure fields.

INTRODUCTION

Swirling radial flows inside ducts appear in many industrial applications such as gas turbine centrifugal compressor diffusers, inter-turbine-ducts, pneumatic devices, etc.

In the last thirty-six years, several papers related to the subject matter have been published. Although one can find earlier contributions, by a number of investigators, dealing with the heat transfer properties in domains similar to the one considered here, we will restrict our short review to contributions that are dealing strictly with isothermal flows. The earlier experiments of Savino and Keshock, 1965, dealt with the experimental determination of velocity and pressure of a sink flow produced in a short cylindrical vortex chamber. Conover, 1968, studied experimentally the laminar flow developed between a rotating disk and a stationary wall with and without radial flow. DeSantis and Rakowsky, 1970, investigated the boundary layer characteristics of the inward fluid motion in a pair of co-axial disks with weak swirl at the inlet. The turbulent source field between two co-rotating disks was the theme of the experimental and theoretical studies of Bake *et al*, 1973.

In this work, a simple but exact method to solve the Navier-Stokes equations in swirling flow configurations is developed. As a model problem, the swirling radial inward flow between two disks of low aspect ratio is considered. The Navier-Stokes equations are cast in terms of the radius times the radial velocity rV_r, and radius times the tangential velocity rV_θ, in cylindrical coordinates. The first variable rV_r is directly proportional to the mass flow rate across any section r and the second variable rV_θ is proportional to the circulation around any circular path of radius r. Given that the disk spacing is small, it is assumed that the shear stress in the radial direction is much larger than that in the axial direction, therefore the latter one is neglected. This simplifies the governing equations, which turn out to be elliptic in the z-direction and parabolic in the radial direction. The shooting method (Keller, 1968) is then used to solve the equations in the z-direction while the implicit Euler backward method is used to integrate the equations in the radial direction. A parametric study is carried out to demonstrate the effect of the Reynolds and the swirl numbers on the flow and pressure fields.

NOMENCLATURE

C	vector defined in Eq. (10)
g	function of z, defined in text as $g(z)=rV_r$
G, F	vectors defined in Eq. (9)
h	disk gap half-height
J	Jacobian matrix, see Eq. (11)
P	pressure
r, θ, z	components of the cylindrical coordinates system

Re	Reynolds number
Re_r	modified Reynolds number, $Re_r=\xi Re$
S	swirl number
u,v,w	variables defined in Eq. (9)
V	velocity component
x	vector defined in Eq. (9)
λ	parameter defined in Eq. (6)
Λ	parameter defined in Eq. (3c)
Ω, ω	swirl rV_θ at r_{i+1} and r_i, respectively
ξ	disk gap height-to-diameter ratio

Subscripts:

i	defers to discrete space location
j	refers to differentiation with respect to x_j
o	reference section, at disk inlet plane
r, θ, z	in the r, θ, or z-direction

Superscripts:

*	dimensional quantity
i	refers to the i^{th} Newton iteration

PROBLEM FORMULATION

Consider the steady, laminar, incompressible, axisymmetric swirling radial flow developed in the gap between a pair of parallel disks that is schematically illustrated in Fig. 1. The continuity and momentum equations that govern this flow, written in cylindrical coordinates, are:

$$\frac{1}{r}\frac{\partial}{\partial r}\left(rV_r\right)=0 \tag{1}$$

$$V_r\frac{\partial V_r}{\partial r}-\frac{1}{r}\left(SV_\theta\right)^2=-\frac{\partial \Delta P}{\partial r}+\frac{1}{\mathrm{Re}_r}\left[\xi^2\frac{\partial}{\partial r}\left(\frac{1}{r}\frac{\partial rV_r}{\partial r}\right)+\frac{\partial^2 V_r}{\partial z^2}\right] \tag{2}$$

$$V_r\frac{\partial rV_\theta}{\partial r}=\frac{1}{\mathrm{Re}_r}\left[\xi^2 r\frac{\partial}{\partial r}\left(\frac{1}{r}\frac{\partial rV_\theta}{\partial r}\right)+\frac{\partial^2 rV_\theta}{\partial z^2}\right] \tag{3a}$$

$$0=-\frac{\partial \Delta P}{\partial z} \tag{4}$$

where $r=r^*/R_o^*$, $z=z^*/h^*$, $\xi=h^*/R_o^*$, $V_r=V_r^*/V_{ro}^*$, $V_\theta=V_\theta^*/V_{\theta o}^*$, $S=V_{\theta o}^*/V_{ro}^*$; V_{ro}^* and $V_{\theta o}^*$ are the average inlet velocities in the radial and tangential directions, respectively; stars indicate dimensional quantities, $\Delta P=\left(P^*-P_o^*\right)/\rho^* V_{ro}^{*2}$, $\mathrm{Re}=V_{ro}^* h^*/\upsilon^*$, and $\mathrm{Re}_r=\xi\,\mathrm{Re}$.

Equations (1) and (4) suggest that:

$$rV_r=g(z) \quad \text{and} \quad \Delta P=\Delta P(r).$$

Leting $rV\theta=\Omega(r,z)$, which is proportional to the circulation, and noting that the spacing between the two disks is much less than one, $\xi<<1$, the r-momentum equation, Eq. 2 can be written as:

$$-\frac{g^2(z)}{r^3}-\frac{1}{r}\left(SV_\theta\right)^2=-\frac{d\Delta P(r)}{dr}+\frac{1}{r\,\mathrm{Re}_r}\frac{d^2 g(z)}{dz^2} \tag{5}$$

which, when ifferentiated with respect to z gives:

$$\frac{d^3 g}{dz^3}+2\lambda^2\left(g\frac{dg}{dz}+S^2\Omega\frac{\partial\Omega}{\partial z}\right)=0 \quad \textit{where} \quad \lambda^2=\mathrm{Re}_r/r^2 \tag{6}$$

Moreover, the θ-momentum equation can be simplified to

$$\frac{g(z)}{r}\frac{\partial\Omega}{\partial r}=\frac{1}{\mathrm{Re}_r}\frac{\partial^2\Omega}{\partial z^2} \tag{3b}$$

The conservation of mass between any two radial sections implies that:

$$\int_0^1 g(z)dz=\pm 1 \tag{7}$$

Where the plus and minus signs represent outflow and inflow, respectively.

The solution for $g(z)$ and $\Omega(r,z)$ is obtained by solving simultaneously a nonlinear coupled system of equations, Eqs. (3b, 6), and satisfying the continuity constraint, Eq. (7), subject to the following initial and boundary conditions:

$$\text{(i)} \quad at \quad r=1\longrightarrow\Omega=1$$

$$\text{(ii)} \quad at \quad z=0\longrightarrow\frac{dg(z)}{dz}=0 \quad and \quad \frac{\partial\Omega(r,z)}{\partial z}=0 \tag{8}$$

$$\text{(iii)} \quad at \quad z=1\longrightarrow g(z)=0 \quad and \quad \Omega(r,z)=0$$

The initial condition (i) implies that the incoming swirl is uniform, while boundary condition (ii) implies symmetry along the mid-plane between the two disks and (iii) implies no slip at the disk upper wall.

NUMERICAL SOLUTION

The numerical procedure, used to solve for the flow in the disk gap, is presented in this section. The conservation equations for continuity and momenta are reduced to two equations for $g(z)$ and $\Omega(r,z)$, namely Eqs. (3b, 6) with the initial and boundary conditions, given in Eqs. (8), and the integral constraint, Eq. (7).

One way to solve this system of coupled nonlinear differential equations is to use the shooting method (Keller, 1968), where these equations are written as a system of nonlinear first order ODE's and the resulting system is solved as an initial value problem using the Runge-Kutta method. Since there are only two conditions to satisfy at the initial point $z=0$, the shooting method (Keller, 1968) is used and is coupled with Newton's method (Isaacson and Keller, 1966) to estimate the other three initial conditions that would simultaneously satisfy the boundary condition at $z=1$, Eqs. (8) and the integral constraint given in Eq. (7). This generally provides quadratic convergence of the iterations and reduces computing time. The Runge-Kutta method is used to integrate the resulting set of first order differential equations as well as the integral

constraint given by Eq. (7). As the set of equations is nonlinear, the solution at any λ and S is obtained by marching in λ and S starting from λ=0 and S=0 until the target values of λ and S are reached.

The above choice of numerical method is justified as follows. In fact, these equations could have been discretized using any of the commonly used methods, e.g. finite difference, finite element, finite volume or spectral collocation method. If we use e.g. the finite difference method to discretize the 3rd order non-linear ODE, Eq. (6), with the boundary conditions, given in Eqs. (8), the resulting system of difference equations will result in a non-linear non-symmetric matrix with a bandwidth of nine/thirteen, if a second/fourth order accuracy is required. The resulting matrix will be ill-conditioned at high Reynolds numbers, hence requiring a direct matrix inversion scheme or an elaborate properly preconditioned iterative solver. Furthermore, the circulation equation, Eq. (3b), and the integral constraint, Eq. (7), have to be simultaneously satisfied, hence some integration scheme has to be adopted to both equations and a method has to be used to couple that constraint with the numerical solution of Eq. (6). It is estimated that, compared to what the authors propose in this work, such an approach will be much more complicated and much more expensive in terms of memory requirements and solution time. In the proposed work, the Runge-Kutta integration scheme is used to integrate both Eqs. (3b,6), (after writing them as a set of five first-order ODE's) as well as the integral constraint, Eq. (7), then the shooting method coupled with Newton scheme provides quadratic convergence to machine zero in 3 to 7 iterations. The details of the chosen numerical method as well as the method used to compute all flow variables are described hereafter.

3.1 The details of the numerical method

Let us note first that the r-momentum equation results in an elliptic equation in the *z*-direction for *g(z)* and the θ-momentum equation results in a heat diffusion type equation for Ω, namely parabolic in the *r*-direction and elliptic in the *z*-direction.

The θ-momentum equation is first discretized in the r-direction using the implicit Euler backward differencing to ensure numerical stability so that, at the current radial location $r=r_{i+1}$, we get:

$$\frac{\partial^2\Omega}{\partial z^2} = \Lambda g\left(\Omega-\omega\right) \tag{3c}$$

where $\Lambda = \dfrac{\mathrm{Re}_r}{r_{i+1}\Delta r}$, $\Delta r = r_{i+1}-r_i$, *and* $\omega = \Omega_i$

In order to solve the problem numerically, continuity and momenta equations were reduced to two differential equations for *g* and Ω, namely Eqs. (3c, 6) with the boundary/initial conditions, Eqs. (8), and the integral constraint, Eq. (7).

Equations (3c, 6) and the initial/boundary conditions, Eqs. (8), are written as a set of five first order ordinary coupled non-linear differential equations:

$$\frac{\partial\vec{G}\left(r_{i+1},z,\vec{x}^{\,i}\right)}{\partial z} = \vec{F} \tag{9}$$

Where

$$\vec{G}=\begin{bmatrix} g\left(z,\vec{x}^{\,i}\right)\\ u\left(z,\vec{x}^{\,i}\right)\\ v\left(z,\vec{x}^{\,i}\right)\\ \Omega\left(r_{i+1},z,\vec{x}^{\,i}\right)\\ w\left(r_{i+1},z,\vec{x}^{\,i}\right)\end{bmatrix},\quad \vec{F}=\begin{bmatrix} u\\ v\\ -2\lambda^2\left(gu+S^2\Omega\omega\right)\\ w\\ g\Lambda\left(\Omega-\omega\right)\end{bmatrix} \text{ and } \vec{x}^{\,i}=\begin{bmatrix} x_1^i\\ x_2^i\\ x_3^i\end{bmatrix}$$

with initial condition $\vec{G}=\begin{bmatrix}x_1^i & 0 & x_2^i & x_3^i & 0\end{bmatrix}^T$.

Given $\vec{x}^{\,i}$ these equations are integrated from the center plane z=0 to the upper disk z=1, using the fourth-order Runge-Kutta method. Since there are only two conditions to satisfy at the initial point z=0, the shooting method, developed by Keller, 1968, is employed so that $\vec{x}^{\,i}$ are the values of $\vec{x}$ at the i^{th} iteration. Newton's method is then used to adjust the solution parameters $\vec{x}^{\,i}$ such that, at convergence, these parameters will satisfy the conditions given in Eqs. (7) and (8) simultaneously. The solution of this initial value problem will be a function of $\vec{x}^{\,i}$, i.e. $G=G\left(r,z,\vec{x}^{\,i}\right)$. Hence we seek $\vec{x}^{\,i}$ such that, at convergence:

$$\vec{C}=\begin{bmatrix} C_1\left(\vec{x}_i\right)\\ C_2\left(\vec{x}_i\right)\\ C_3\left(\vec{x}_i\right)\end{bmatrix}=\begin{bmatrix} g\left(z=1,\vec{x}_i\right)\\ \int_0^1 g\left(z,\vec{x}_i\right)dz\pm 1\\ \Omega\left(r,z=1,\vec{x}_i\right)\end{bmatrix}=\begin{bmatrix}0\\0\\0\end{bmatrix} \tag{10}$$

and $\pm$ correspond to inflow/outflow. Newton's method, see Isaacson and Keller, 1966, is then used to obtain a better guess for $\vec{x}^{\,i}$ as follows:

$$\Delta\vec{x}=-\left[J\right]^{-1}\vec{C} \quad where \quad \left[J\right]=\left(\frac{\partial C_i}{\partial x_j}\right)_{at\ z=1} \tag{11}$$

where i and/or j = 1, 2, 3, and $\Delta\vec{x}^{\,i}=\vec{x}^{\,i+1}-\vec{x}^{\,i}$.

The terms involved in the Jacobian matrix, which contain $\partial g/\partial x_j$ and $\partial\Omega/\partial x_j$, are obtained by differentiating Eqs.(5) with respect to x_j, where j=1, 2, 3, to give:

$$\frac{\partial\vec{G}_j\left(z,\vec{x}^{\,i}\right)}{\partial z}=\vec{F}_j$$

$$where\ \vec{G}_j=\frac{\partial\vec{G}}{\partial x_j}\ \ and\ \ \vec{F}_j=\begin{bmatrix} u_j\\ v_j\\ -2\lambda^2\left(g_ju+u_jg+S^2\Omega_j\omega\right)\\ w_j\\ \Lambda\left(g_j\Omega+g\Omega_j\right)\end{bmatrix} \tag{12}$$

with initial conditions, for j = 1, 2, 3:

$\vec{G}_1=\begin{bmatrix}1 & 0 & 0 & 0 & 0\end{bmatrix}^T$, $\vec{G}_2=\begin{bmatrix}0 & 0 & 1 & 0 & 0\end{bmatrix}^T$, $\vec{G}_3=\begin{bmatrix}0 & 0 & 0 & 1 & 0\end{bmatrix}^T$

Once the velocity field is calculated as described hereafter, the pressure difference between the current section and the reference one is obtained by integrating Eq. (5) between *r*=1

and $r=r_{i+1}$, and noting that, along the disk walls, both velocities vanish identically, hence

$$\Delta P = \frac{1}{\mathrm{Re}_r}\int_1^r \frac{1}{r}\left(\frac{\partial^2 g}{\partial z^2}\right)_{z=1} dr = \frac{1}{\mathrm{Re}_r}\int_1^r \frac{1}{r} v_{z=1} dr$$

For a given value of λ, the solution at any radial location, r_{i+1}, proceeds as follows:

a. Assuming an initial guess $\vec{x}^o$ solve simultaneously the sets of first order differential equations for $\vec{G}$ *and* $\vec{G}_j$ using the fourth-order Runge-Kutta method.
b. Calculate $\vec{x}^{i+1}$ from Eqs. (11)
c. Repeat steps a and b until the L_2 norm of the error $\Delta\vec{x}$ is less than 10^{-10}
d. Move to the next radial location and repeat steps a, b, c

For large values of λ and/or *S* the equations are strongly nonlinear and a good initial guess of $\vec{x}^o$ becomes crucial. In this case, the solution is obtained by marching first in λ from zero to the final value, then marching in *S* from zero to the final value. At the starting point, λ=0 and *S*=0, the initial guess $\vec{x}^o$ is set to zero and the procedure described above is implemented until convergence. The limit of λ=0 is in fact the creeping flow limit where the flow equations are linear. The value of λ is then incremented and the current value of $\vec{x}^i$ is used as initial guess, then λ is incremented again and so on until the target λ value is reached. The same process is then repeated for *S*.

RESULTS AND DISCUSSION

A parametric study was carried out to show the effect of the different parameters on the resulting flow field and pressure distribution. The effect of Reynolds number *Re* and swirl number *S*, on the flow and pressure fields is presented in this section.

Figures 2.a,b give the flow development as well as the radial and axial velocities in the disk gap for a Reynolds number *Re*=25, a gap height ξ=1/9, and a swirl number *S*=15. The first observation is the radial velocity defect in the core flow due to centrifugal effects, which is balanced by a velocity overshoot near the walls, where V_θ is small, creating a strong shear layer flow. This effect is also confirmed in Fig. 3, which shows that a larger centrifugal force associated with a larger swirl number results in a shift in the maximum radial velocity from the disk center line to the periphery where the tangential velocity (hence centrifugal force) is much smaller due to viscous effects. Savino and Keshock, 1965, also observed this behavior experimentally.

Figures 4 and 5 show the effect Reynolds number on the flow. Figure 4 shows the effect of Reynolds number on the radial and tangential velocities at the center-line of the disk inlet plane. For the same Re, as the swirl number increases, the C.L. radial velocity decreases. As the Reynolds number increases, the tangential velocity diffuses less and the corresponding radial velocity tends to decrease. In Figs. 5.a-d, the radial and tangential velocities along the gap centerline, between r=1 and r=0.3 are plotted for different Reynolds numbers. For Re=2.5, which is approaching a creeping flow, the tangential velocity (and hence the centrifugal force) diffuses rather rapidly, which explains the fact that the radial velocity approaches that of a non-swirling flow as the radius decreases. Figure 6 shows that, for a given swirl, an increase in Reynolds number has an effect on the radial velocity profile, which is similar to increasing the swirl number for a given Reynolds number. Figure 7 shows that, for small Reynolds numbers, the swirl diffuses from 1 to 0.5 between r=1 and r=0.9 and is about 0.25 at r=0.8. This explains the fact that the radial velocity profile approaches that of a non-swirling flow case as the flow moves inwards. Figure 8 shows the effect of the centrifugal force on the pressure coefficient.

The results indicate that, above a certain Reynolds number, the diffusion of circulation in the radial direction is rather negligible and the velocity overshoot near the disk walls becomes more pronounced as the radius decreases. The exact opposite occurs when Reynolds number is around one, i.e. the diffusion of circulation is so strong that the radial velocity profiles approach that of a non-swirling flow as the radius decreases.

CONCLUSION

The flow in a low aspect ratio vortex chamber has been modeled with a unidirectional flow between two concentric disks. The Navier-Stokes equations were reduced into two equations for the radial and axial velocity, which were simultaneously solved using the shooting method coupled with Newton method.

A parametric study of the effect of Reynolds number and the swirl number on the flow field and pressure distribution showed that the flow pattern in very sensitive to the swirl number. For creeping flows where Reynolds number is around one, the swirl diffuses rather rapidly and the flow pattern approaches that of a purely radial inward flow. Above a certain Reynolds number, the diffusion of swirl is rather negligible and a strong shear layer flow develops near the disk walls where the velocity overshoots whereas it undershoots in mid-passage where the velocity is vanishingly small or reversed flow exists. These trends were also observed experimentally.

REFERENCES

Conover, R.A., 1968, "Laminar Flow Between a Rotating Disk and a Parallel Stationary Wall with and without Radial Flow". J. Basic Eng., Transactions of ASME., pp. 325-332, Sept. 1968.

DeSantis, M. J. and Rakowsky, E. L., 1970, "An Experimental Investigation of the Viscous Flow Field in a Pneumatic Vortex Rate Sensor", ASME Fluidics Conference, Atlanta, GA, June 22-23, 1970.

Dakke, E., Kreider, J.F., and Kreith, F., 1973, "Turbulent Source Flow Between Parallel Stationary and Co-Rotating Disks". J. Fluid Mech., vol. 58, part 2, 1973, pp 209-231.

Isaacson, E. and Keller, H.B., 1966, "Analysis of Numerical Methods", John Wiley and Sons, New York 1966.

Keller, H.B., 1968, "Numerical methods for two-point boundary value problems", Ginn-Blaisdell, Waltham, Mass, 1968.

Savino, J.M., and Keshock, E.G., 1965, "Experimental Profiles of Velocity Components and Radial Pressure Distributions in a Vortex Contained in a Short Cylindrical Chamber", NASA TN D-3072, October 1965.

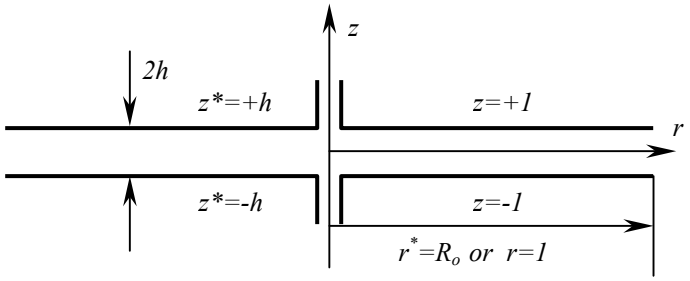

Figure 1 Schematic diagram of the problem

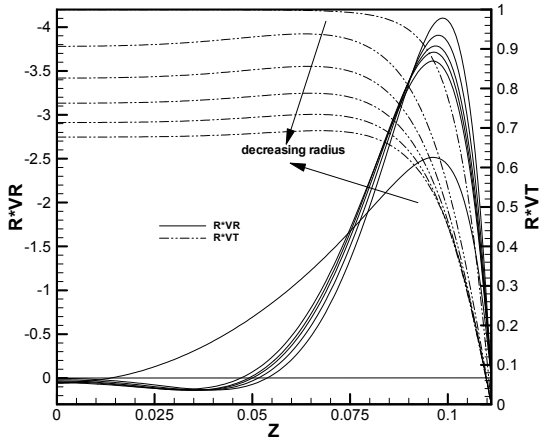

Figure 2.a The radial and tangential velocity profiles at r=1, 0.9, … , 0.5

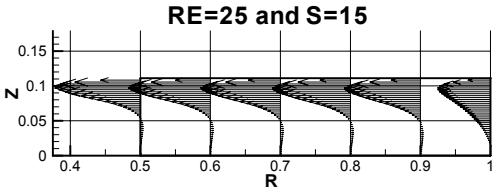

Fig 2.b The flow field for Reynolds number Re=25 and swirl number S=15

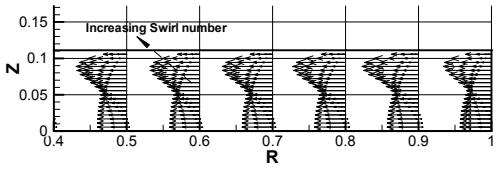

Figure 3. The flow field for Re=10 and swirl numbers S=0, 5, 10, and 15

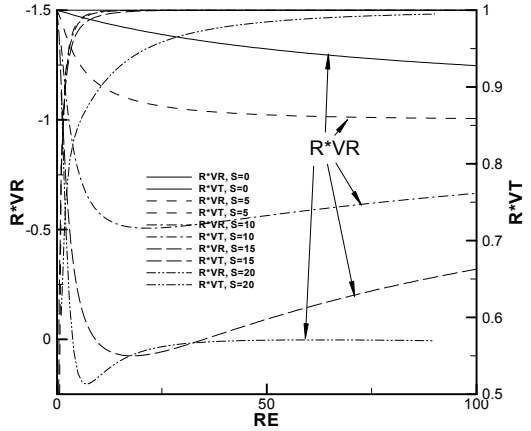

Figure 4. Velocities along C.L. of disk inlet plane for different swirl numbers

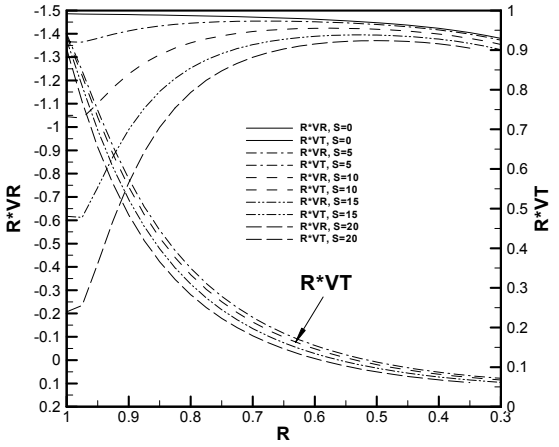

Figure 5.a C.L. velocities for Re=2.5

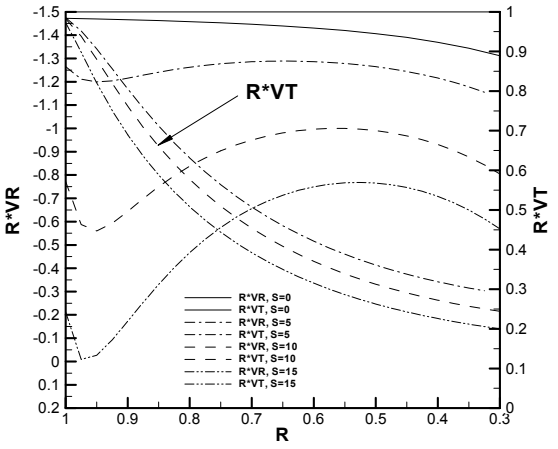

Figure 5.b C.L. velocities for Re=5

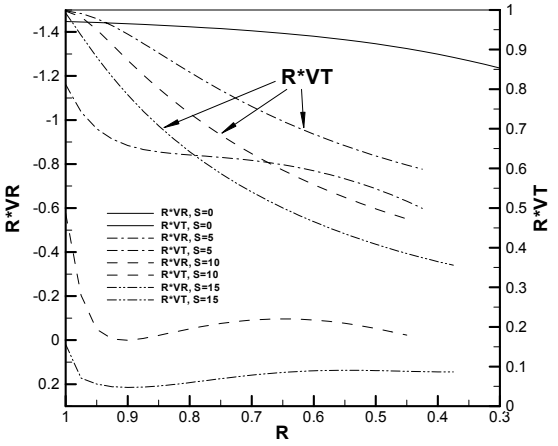

Figure 5.c C.L. velocities for Re=10

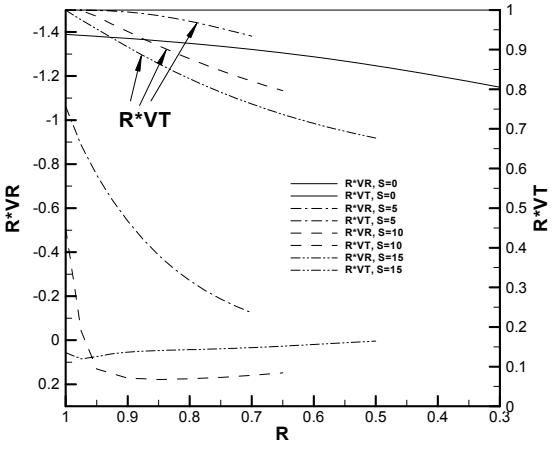

Figure 5.d C.L. velocities for Re=25

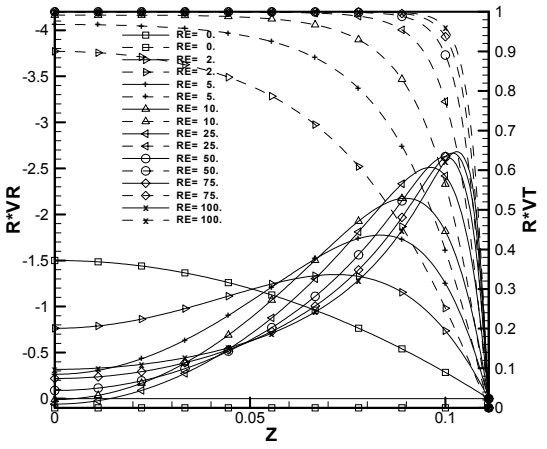

Figure 6 The velocities at disk inlet for a swirl number S=15

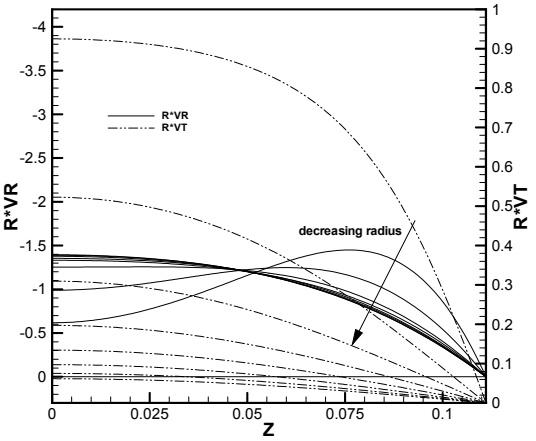

Figure 7. The velocities at r=1, 0.9, … , 0.3, for Re=2.5 and S=15.

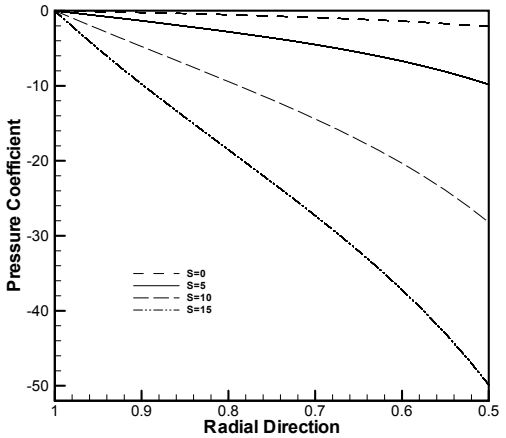

Figure 8. The pressure coefficient for Re=10 and different swirl numbers, for a gap height=1/9